Dynamical Jahn-Teller effect and fluorescence line narrowing of the $^4A_2$-$^4T_2$ zero-phonon transition in $KZnF_3$:Cr

O. Pilla, E. Galvanetto, M. Montagna, and G. Viliani
Dipartimento di Fisica, Università di Trento, 38050 Povo, Trento, Italy
(Received 11 December 1987; revised manuscript received 24 March 1988)

Fluorescence-line-narrowing measurements of the $^4A_2$-$^4T_2$ zero-phonon line of $KZnF_3$:Cr are reported. The structure of the spin-orbit-split line is studied on the basis of a single-mode approximation, including Jahn-Teller coupling to tetragonal modes. The results are compared with those of other, similar systems, and the validity of the single-mode model is discussed.

I. INTRODUCTION

The theory of the dynamical Jahn-Teller effect (DJTE) in isolated impurities in ionic crystals was developed by Ham,[1] who showed that nondiagonal electronic operators (e.g., spin-orbit interaction) are quenched even when the coupling is not strong enough to distort the impurity environment. Another observable consequence of the DJTE is the selective intensity quenching it produces on different spin-orbit (s.o.) components of a zero-phonon line (ZPL).[2,3]

Model systems for the observation of such effects are the d^3 impurities in cubic crystals, because the JTE is comparable to the s.o. interaction and both are of intermediate strength so that s.o.-split ZPL's can be observed. The Ham quenching of s.o. interaction was first observed and studied by Sturge[4] in $KMgF_3$:V; the data of Ref. 4 were used in Ref. 2 in order to fit the JT-quenched relative intensities of the $^4A_2$-$^4T_2$ s.o. components within the single-mode model.

This system seems to have been the only one where the theory of Refs. 1 and 2 can be easily applied; in fact, other apparently simple systems such as MgO:V, MgO:Cr, and ruby suffer from the fact that $^4T_2$ is not the first excited state. As a consequence, fast nonradiative decay to the lower-lying level (^2E) takes place and (due to the interaction with the phonon continuum) the s.o. components of $^4T_2$ are (homogeneously) very broadened and Lamb shifted.[5-7] Therefore, it seems worthwhile to study a different system where $^4T_2$ is the first excited state, so that the theoretical predictions can be checked. In fact, as already pointed out by Rorison and O'Brien,[8,9] the use of the single-mode model may not be appropriate when one tries to fit both the splittings and the intensities.

The system under investigation in the present paper is $KZnF_3$:Cr^{3+}, which is also interesting from a technological point of view since true cw-laser operation has been achieved at room temperature.[10] The Cr ion substitutes for Zn^{2+} (cubic site), thus requiring charge-compensating vacancies; as a result, in addition to the cubic Cr centers, Cr ions with lower symmetry, namely, tetragonal (Zn vacancy in the [001] directions) or trigonal (K vacancy in the [111] directions), can exist.[11,12] Moreover, the vacancies also affect the so-called cubic centers, and small distortions result in inhomogeneous ZPL broadening. Thus, in order to be able to study the DJTE it was necessary to perform fluorescence-line narrowing (FLN) in order to select among the nearly cubic centers.

In the next sections we report on the experimental results concerning the Ham and intensity-quenching effects, and on the role of the low-energy acoustical phonons in the homogeneous broadening of the lines.

II. EXPERIMENTAL RESULTS

The pale-green samples ($\approx 2\times 3\times 3$ mm^3) had good optical quality and were provided by U. Dürr; the Cr doping was performed by adding $CrCl_3$; Cr concentration was 5000 ppm. Excitation was by a He-Ne laser for emission spectra, and either by an excimer-pumped Lambda-Physik FL 2001 dye laser (spectral resolution ≈ 0.3 cm^{-1}) or a lamp plus monochromator, for high- and low-resolution excitation spectra, respectively. The sample was placed in a variable-temperature cryostat (2–300 K), and luminescence was observed at right angles and dispersed in a Spex 1401 double monochromator (maximum resolution ≈ 0.15 cm^{-1}). Time-resolved photon-counting detection was employed in order to avoid directly scattered laser light. Lifetime measurements on the emission lines corresponding to differently distorted centers were also carried out, and they are in general agreement with previous data.[11]

In Fig. 1 we report the absorption spectrum at room temperature where the predicted energies of some levels of cubic Cr^{3+} are indicated, even though the spectrum results from the superposition of absorption from centers of all symmetry. As can be seen from the emission spectrum of Fig. 2, three ZPL's are observed at 4.2 K, which are thought to correspond to the three types of centers mentioned above: the A line to trigonal centers (lifetime ≈ 0.22 ms), B to cubic centers (lifetime ≈ 0.46 ms), and C to tetragonal ones (lifetime ≈ 0.46 ms). The shorter lifetime value of A agrees qualitatively with the symmetry assignment, since the transition is electric-dipole forbidden in cubic symmetry. Moreover, by monitoring the ZPL emission lines under FLN conditions, we observe a well-resolved triplet structure (with splitting of ≈ 0.35 cm^{-1}) for the trigonal A line which is due to ground-level

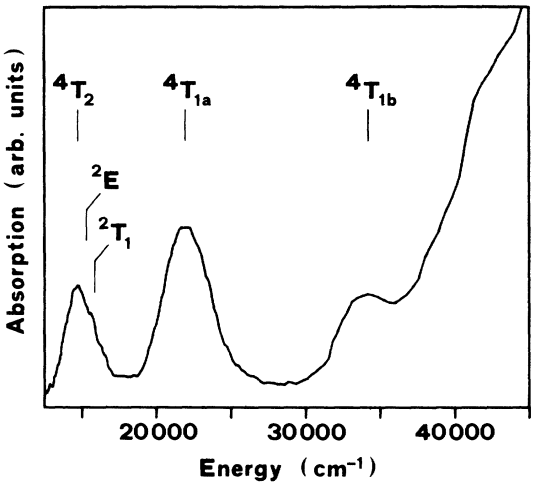

FIG. 1. Absorption spectrum of $KZnF_3$:Cr at room temperature. The labels refer to the calculated positions of relevant energy levels of cubic Cr ions.

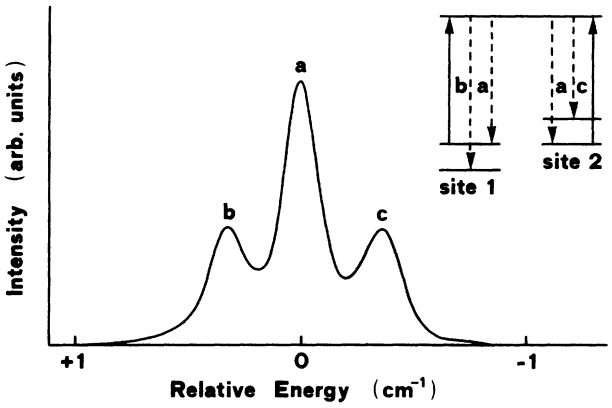

FIG. 3. FLN spectrum of the trigonal A line at 4.2 K. Two sets of centers are resonantly excited within the inhomogeneous profile; the triplet structure is due to the 0.35-cm^{-1} splitting of the $^4A_2$ ground state.

splitting (see Fig. 3), a broadening of the line C, and no measurable effect on the cubic B line. EPR data,[13] provide zero-field splittings of 0.32 (trigonal), 0.1 (tetragonal), and 0 (cubic) cm^{-1}. However, the assignment of C to tetragonal centers is not unequivocal. In fact, its lifetime coincides with the cubic one, and its intensity relative to A and B is very different from the relative concentration of tetragonal centers as deduced from EPR in Ref. 13; moreover, its excitation spectrum is extremely similar to that of B.

The low-resolution excitation spectrum of the cubic B line at 4.2 K is reported in Fig. 4, showing the two broad bands corresponding to $^4T_2$ and $^4T_1$. The dips indicated by the arrows are attributable to Fano resonances between the $^4T_2$ band and the $^2E, ^2T_1$ spin-forbidden transitions.[14]

The quartet structure of the $^4T_2$ cubic ZPL has been observed in absorption by Brauch[15] at liquid-helium temperature, but the quartet is superimposed on the absorption bands due to the other centers. In this situation it is more convenient to record high-resolution (both in excitation and in emission) excitation spectra of cubic centers; this technique allows the contribution of cubic centers to be singled out and, moreover, allows for site selection by observing different energies within the inhomogeneous ZPL (Fig. 5).

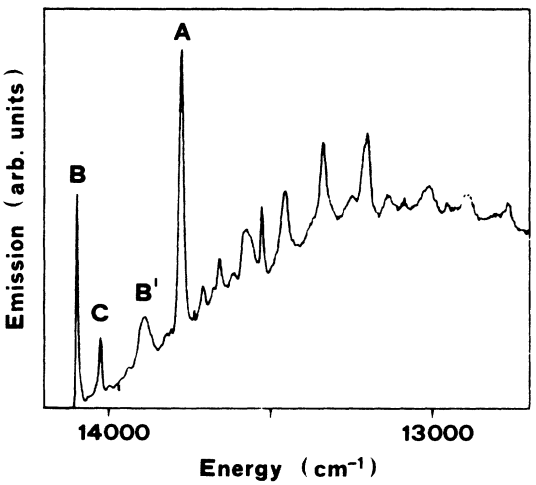

FIG. 2. Emission spectrum at 4.2 K. The lines labeled B and A correspond to the zero-phonon lines of cubic and trigonal centers, respectively; B' is the first phonon replica of the cubic emission; C is thought to derive from tetragonal centers (see text).

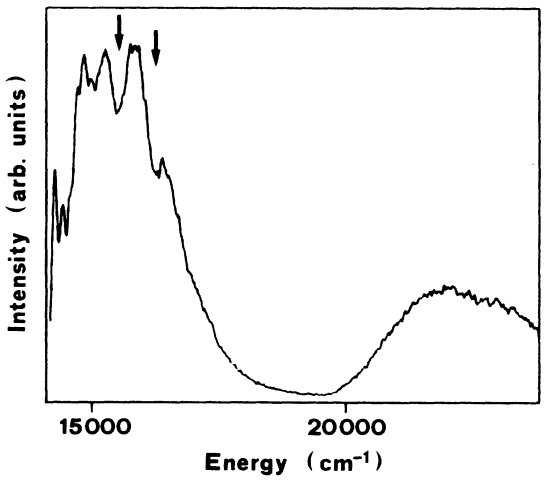

FIG. 4. Low-resolution excitation spectrum of the cubic centers emission (B) at 4.2 K (not corrected for system response). The two broad bands correspond to the spin allowed $^4T_2$ and $^4T_1$ levels. The dips indicated by the arrows are attributed to Fano resonances between the ^2E and $^2T_1$ levels and $^4T_2$.

Figure 5(a) shows the excitation spectrum of the phonon sideband of the cubic emission (B' peak of Fig. 2). The inhomogeneously broadened $^4A_2$-$^4T_2$ zero-phonon spin-orbit quartet is clearly observed; the peaks are labeled according to O_h double-group irreducible representations: Γ_7, which corresponds to line B in Fig. 2, is asymmetric with an extended tail towards low energies.

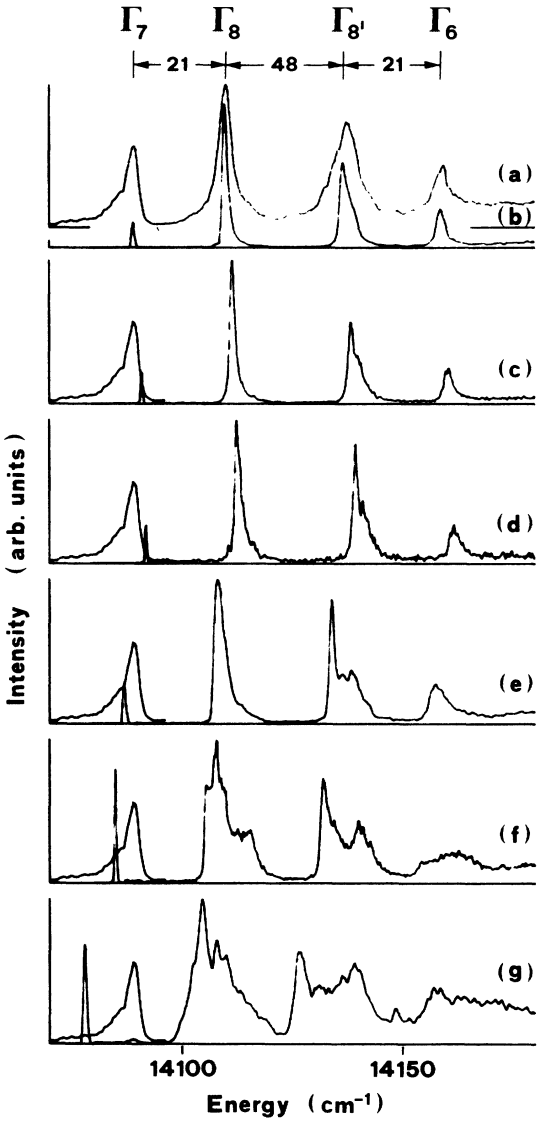

FIG. 5. (a) Excitation spectrum of the B' peak of Fig. 2 in the $^4T_2$ ZPL range, the inhomogeneously broadened quartet is shown and peaks are labeled according to their symmetry. Traces (b)–(g) are the FLN excitation spectra taken at different energies within the Γ_7 emission line; the inhomogeneously broadened Γ_7 excitation profile (which is identical to the emission one) is superimposed to all spectra in order to show the detection wavelength. Energy differences between detection wavelength and line center are as follows: (cm^{-1}): (b) 0, (c) +2, (d) +3, (e) −2, (f) −4, and (g) −11. The intensities of the resonant peaks in spectra (b)–(g) have been divided by a factor of 10. The splittings reported on the top of the figure are relative to trace (b), i.e., nearly cubic centers.

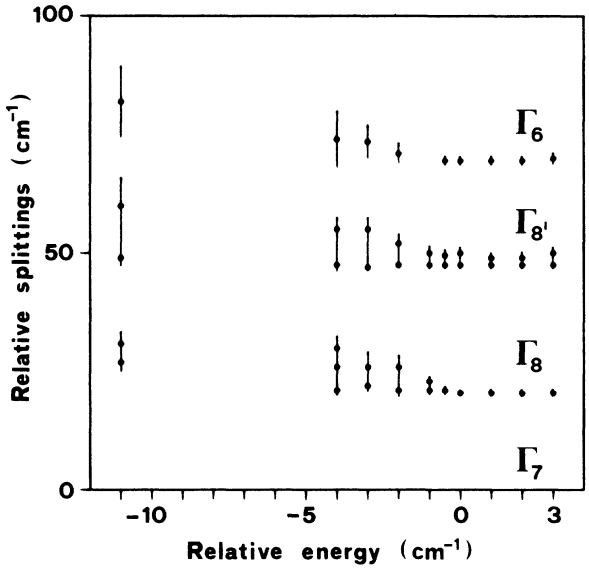

FIG. 6. Splittings of the $^4T_2$ ZPL's (relative to the Γ_7 level) as a function of the energy shift from the inhomogeneous line center, as deduced from the spectra of Figs. 5(b)–5(g). The dots correspond to the main peaks, the bars give a rough estimate of the overall width of the structures. The symmetry (cubic terminology) is also reported.

In Figs. 5(b)–5(g) we report the corresponding FLN spectra obtained by detecting at different energies within the B (Γ_7) emission line. We note that spectra 5(b), 5(c), and 5(d) are narrower than those taken by detecting in the low-energy side of B (Γ_7), i.e., 5(e), 5(f), and 5(g), where more structures are also present. This behavior clearly indicates that several centers are present at slightly perturbed cubic sites: nearly cubic centers emit in the high-energy wing of Γ_7, while Cr ions placed at more distorted environments fluoresce at lower energies. This agrees with the general fact that the distorted centers emit at lower energy.

The rather puzzling shape of the (f) and (g) spectra is due to two effects: (i) in lower-than-cubic symmetry the two (fourfold degenerate) Γ_8 peaks are split, giving rise to a sixfold structure of the ZPL; (ii) the residual inhomogeneous broadening is more important, i.e., differently perturbed centers fluoresce at the same energy.

The above considerations are summarized in Fig. 6, where the bars roughly indicate the widths of the structures, and the dots the peak positions relative to Γ_7. In passing from higher energies to the center of the emission line no changes are observed in splittings and widths, while there are drastic variations when we select emission in the low-energy wing: the overall splitting increases from 69 up to ≈ 80 cm^{-1}, and several peaks are observed in the Γ_8-$\Gamma_{8'}$ range.

III. DISCUSSION

The study of the structure of the cubic $^4T_2$ ZPL requires the knowledge of several parameters, namely, the

$10Dq$ crystal-field parameter, the covalence-quenched free-ion parameters B, C and the s.o.-coupling coefficient ζ, the Jahn-Teller coupling constant, and the effective phonon frequency. Moreover, it is more convenient to use an effective s.o. Hamiltonian[16,17] which introduces two more s.o. coupling constants

$$H_{\text{s.o.}} = \lambda L * S + \mu(L * S)^2 + \rho(L_x^2 S_x^2 + L_y^2 S_y^2 + L_z^2 S_z^2) , \quad (1)$$

where L is the effective angular momentum ($L=1$) for a T_2 state.

As concerns the choice of the parameters, $10Dq$ was deduced from the energy of the $^4T_2$ absorption band, yielding 14 900 cm^{-1}. The effect of the covalence on the free-ion parameters was evaluated by fitting the absorption spectrum with only one adjustable parameter;[18,19] the following values were obtained: $\zeta=217$ cm^{-1}, $B=725$ cm^{-1}, and $C=3265$ cm^{-1}, which are the free-ion values[20] reduced by a factor of 0.79. In this way we fit the maximum of the absorption bands, but in order to find the splittings of the $^4T_2$ ZPL, we diagonalize the d^3 matrix with $Dq=13\,300$ cm^{-1}, which is appropriate for emission.[21] The energies of the $^4T_2$ spin-orbit sublevels so obtained are fitted by the effective Hamiltonian (1), which determines the new s.o. parameters $\lambda=30.2$ cm^{-1}, $\mu=7$ cm^{-1}, and $\rho=-21.8$ cm^{-1}.[21,22]

We now introduce the DJT coupling to ϵ_g modes within the $^4T_2$ level so that, assuming coupling to only one mode, the effective Hamiltonian becomes

$$H = H_{\text{s.o.}} + H_{\text{vib}} + b(Q_\epsilon E_\epsilon + Q_\theta E_\theta) , \quad (2)$$

where H_{vib} is the energy of the nuclei, the Q's are the tetragonal coordinates, the E's are the matrices given by Ham, Ref. 1, and b is the Jahn-Teller coupling constant. Hamiltonian (2) was diagonalized including six vibrational states for various values of b and of the vibrational quantum, $\hbar\omega$. Neglecting trigonal modes is justified because the latter are expected to be much less coupled.[18]

In Fig. 7 we report the $^4T_2$ energy levels (relative to Γ_7) as a function of the ratio $R=E_{\text{JT}}/\hbar\omega$, for two values of $\hbar\omega$. As can be seen R is the only relevant parameter, even though high values of $\hbar\omega$ seem to shift Γ_8 slightly in the right direction. The best fit to the experimental splittings yields $R=0.6$. As regards the intensities, they are reported in Fig. 8 for $R=0.6$ and as a function of $\hbar\omega$. In fact, as discussed in Ref. 2, the intensities strongly depend on the value of the vibrational quantum and do not depend very much on R if R is greater than ≈ 0.5. The best fit is obtained for $\hbar\omega=220$ cm^{-1}, yielding in turn $E_{\text{JT}}\approx 130$ cm^{-1}.

The agreement with the experiment is rather good, as in the case of the splittings, and one would be lead to conclude that the one-mode model well reproduces both the splittings and the intensities with $\hbar\omega=220$ cm^{-1} and $E_{\text{JT}}\approx 130$ cm^{-1}.

However, this procedure may underestimate E_{JT}. In fact, in principle one should consider the whole density of vibrational states which couple to the impurity, which in this case extends up to ≈ 500 cm^{-1}. Since the intensities

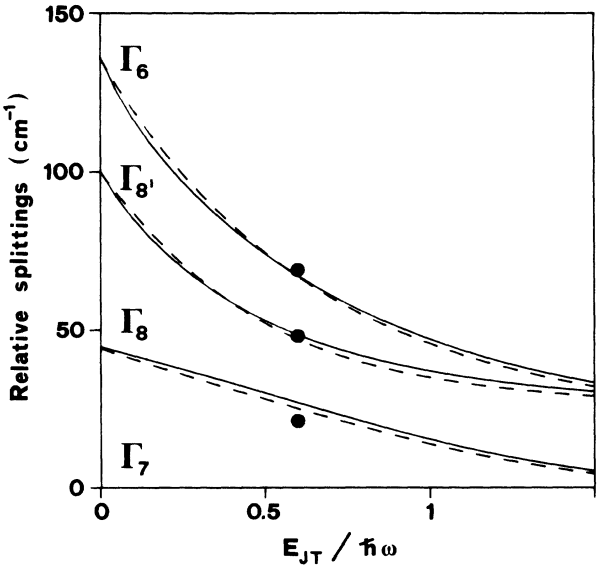

FIG. 7. Splitting of the $^4T_2$ ZPL relative to the lowest Γ_7 state as a function of the ratio $E_{\text{JT}}/\hbar\omega$; solid line, $\hbar\omega=150$ cm^{-1}; dashed line, $\hbar\omega=500$ cm^{-1}. The dots correspond to the experimental splittings ($E_{\text{JT}}/\hbar\omega\approx 0.6$).

are very sensitive to the effect of low-energy acoustic phonons, which induce a higher mixing between the zero-phonon states and the sideband,[2] the effective frequency that one obtains by fitting the intensities will be shifted towards the low-energy side of the density of states. On the other hand, as shown by the discussion reported in Ref. 9, high-frequency phonons give the major contribution to the JT stabilization energy. Therefore, in the presence of a broad density of JT active vibrations, the

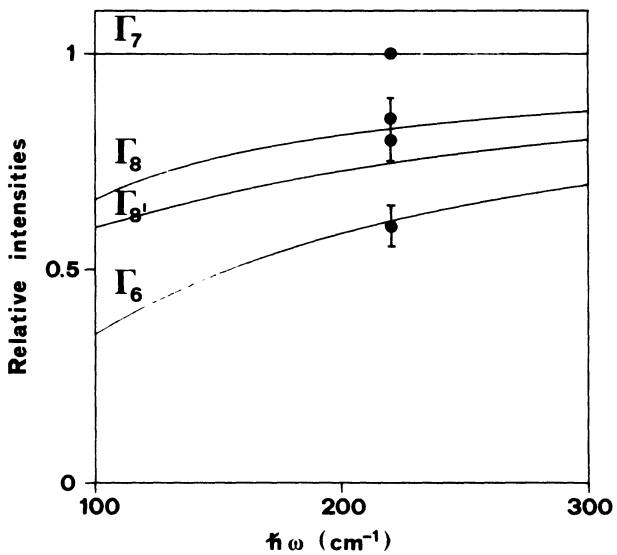

FIG. 8. Intensities (relative to Γ_7) of the $^4T_2$ ZPL sublevels for $E_{\text{JT}}/\hbar\omega=0.6$ as a function of the phonon energy. The intensities are normalized to the degree of degeneracy of the levels. The experimental ratios are shown by the dots ($\hbar\omega\approx 220$ cm^{-1}).

effective value of $\hbar\omega$ which reproduces the intensities is expected to underestimate the JT stabilization energy. A semiquantitative estimate of this effect may be obtained by calculating the relative relevance of the coupling to modes of different symmetry. Experimentally the total Stokes shift of the $^4A_2$-$^4T_2$ transition, as deduced from the emission and excitation spectra, is $\sim 800\ \mathrm{cm}^{-1}$. Taking $E_{JT} = 130\ \mathrm{cm}^{-1}$ the relative contribution of ϵ_g modes would be of only $\frac{1}{6}$. By using the angular overlap method as developed by Bacci[23,24] the electron-phonon coupling and elastic constants can be expressed in terms of the first and second spatial derivative of the Cr-F overlap integrals. In this way we obtain nearly equal contributions to the Stokes shift from a_{1g} and ϵ_g modes (both of the order of $500\ \mathrm{cm}^{-1}$), while the trigonal modes are found to be at least 1 order of magnitude less coupled.

Another indication that the values obtained by the single-mode model are not completely satisfactory, is that a slightly improved fitting of the splittings is obtained with higher values of the vibrational quantum (see Fig. 7).

In any case, it is unquestionable that in this system the single-mode model works better than it does in MgO:V and $KMgF_3$:V, where an unrealistically low value of $\hbar\omega$ is required in order to fit the intensities. Nevertheless, from the previous discussion it turns out that even in the present more favorable case, the single-mode model should be taken with some caution.

In Ref. 9 a two-mode calculation led to improved agreement for MgO:V, and showed in detail the difficulties of the single-mode model in simulating the effects of the actual density of states, where the low-frequency phonons are so important in determining the intensities.

Acoustical low-frequency phonons play another important role in broadening the ZPL's by relaxation within the s.o. multiplet. Actually, even at 4.2 K (see Fig. 5) the higher-energy components are superimposed on a low but detectable and increasing background and the Fano-type discrete-continuum interaction[5,6] is expected to broaden them. However, the presence of residual inhomogeneous broadening precludes even a qualitative analysis of this effect at low temperature. Preliminary data on the temperature induced broadening of Γ_7 in the range 4.2–40 K show a progressive broadening of the line, whose temperature behavior is qualitatively accounted for by a direct process; the broadening is of course Jahn-Teller assisted mainly through $\Gamma_7 - \Gamma_{8'}$ mixing.

ACKNOWLEDGMENTS

We wish to thank U. Dürr for providing the samples and for useful discussions, and M. Bacci for his patience in teaching us the angular overlap method. This work was partially supported by the CISM.

[1]F. S. Ham, Phys. Rev. **138**, A1727 (1965).
[2]M. Montagna, O. Pilla, and G. Viliani, J. Phys. C **12**, L699 (1979), and references therein.
[3]S. Muramatsu and N. Sakamoto, J. Phys. Soc. Jpn. **46**, 1273 (1979).
[4]M. D. Sturge, Phys. Rev. B **1**, 1005 (1970).
[5]M. Montagna, O. Pilla, and G. Viliani, Phys. Rev. Lett. **45**, 1008 (1980).
[6]O. Pilla, M. Montagna, and G. Viliani, Phys. Rev. B **24**, 666 (1981).
[7]M. Ferrari, M. Montagna, O. Pilla, S. Santucci, and G. Viliani, Phys. Rev. B **25**, 3063 (1982).
[8]J. Rorison, Ph.D. thesis, University of Oxford, 1984 (unpublished).
[9]J. Rorison and M. C. M. O'Brien J. Phys. C **17**, 6723 (1984).
[10]U. Brauch and U. Dürr, Opt. Lett. **9**, 441 (1984).
[11]U. Brauch, Ph.D. thesis, University of Stuttgart, 1983 (unpublished).
[12]U. Brauch and U. Dürr, Opt. Commun. **49**, 61 (1984), and references therein.
[13]J. L. Patel, J. J. Davies, B. C. Cavenett, H. Takeuchi, and K. Horai, J. Phys. C **9**, 129 (1976).
[14]M. D. Sturge, H. J. Guggenheim, and M. H. L. Pryce, Phys. Rev. B **2**, 2459 (1970).
[15]U. Brauch (unpublished).
[16]J. Kanamori, Prog. Theor. Phys. **17**, 177 (1957).
[17]P. Koidl, Phys. Status Solidi B **74**, 477 (1976).
[18]G. Viliani, O. Pilla, M. Montagna, and A. Boyrivent, Phys. Rev. B **23**, 18 (1981).
[19]J. C. Eisenstein, J. Chem. Phys. **34**, 1628 (1961).
[20]S. Sugano, Y. Tanabe, and H. Kamimura, *Multiplets of Transition-Metal Ions in Crystals* (Academic, New York, 1970).
[21]For the correct choice of $10Dq$, see Ref. 4 and Note 35 in Ref. 20.
[22]The position of ^2E was determined by emission under hydrostatic pressure, O. Pilla (unpublished).
[23]M. Bacci, Chem. Phys. **40**, 237 (1979).
[24]M. Bacci, Phys. Status Solidi B **92**, 193 (1979).